

Antimalarial Activity and Toxicity of a Novel Chitosan Schiff-Base Scaffold of Aloin Isolated from *Aloe Barbadensis*

Caroline K. Nakiguli ^{1,2} , Viola J. Kosgei ^{1,*}, John Odda ³, Timothy Omara ^{4,*} , Clement O. Ajayi ⁵ , Jackson K. Cherutoi ¹

¹ Department of Chemistry and Biochemistry, School of Sciences and Aerospace Studies, Moi University, Eldoret, Kenya; jcherutoi@mu.ac.ke (J.K.C.);

² Department of Chemistry, Faculty of Science, Mbarara University of Science and Technology, Mbarara, Uganda; cnakiguli@must.ac.ug;

³ Department Pharmacology and Therapeutics, College of Health Sciences, Makerere University, Kampala, Uganda; jodda@ciu.ac.ug;

⁴ Department of Chemistry, College of Natural Sciences, Makerere University, Kampala, Uganda

⁵ Pharm-Biotechnology and Traditional Medicine Center (PHARMBIOTRAC), Mbarara University of Science and Technology, Mbarara, Uganda; cajayi2013@yahoo.com;

* Correspondence: viokos84@yahoo.com (V.J.K.); prof.timo2018@gmail.com, timothy.omara@mak.ac.ug (T.O.);

Received: date; Accepted: 11.04.2025; Published: 30.09.2025

Abstract: Aloin, an anthraquinone-C-glycoside found in *Aloes*, exhibits antimalarial activity; however, its development into therapeutic drugs is hindered by its intrinsic chemical instability. Herein, we synthesized a novel and stabilized the chitosan-Schiff base of aloin (ALCSB) through superficial Schiff condensation of chitosan's amino groups with 2-chloroquinoline-3-carbaldehyde. The aloin was extracted from *Aloe barbadensis* leaf latex, identified, and quantified using high-performance liquid chromatography with an authentic standard. The synthesized ALCSB was characterized using ultraviolet-visible spectroscopy, which showed distinct absorption bands between 258 nm and 368 nm, indicating successful structural modification. These were supported by Fourier-transform infrared spectroscopy analysis revealing characteristic shifts and new bands corresponding to imine and carbonyl functional groups. Scanning electron micrographs depicted a smoother morphology for ALCSB compared to the rugged structure of raw aloin, while thermogravimetric analysis demonstrated enhanced thermal stability of ALCSB compared to aloin and the chitosan-Schiff base. In antimalarial efficacy tests against *Plasmodium berghei* NK65-infected mice, all the doses of ALCSB significantly inhibited parasitemia when compared with the control and the aqueous extract ($P < 0.05$). The highest ALCSB dose tested (1000 mg/kg) had the highest parasitemia suppression of 79.73%. Both aloin and ALCSB had a median lethal dose of 1,103 mg/kg, although 11% of the mice administered with aloin at 2,000 mg/kg died within the first 6 h, indicating that it was more toxic. Thus, the derivatization of aloin using the chitosan-Schiff base enhanced its antimalarial efficacy while reducing the toxicity.

Keywords: *Aloe vera*; chitosan; malaria phytotherapy; scaffold; traditional medicine.

© 2025 by the authors. This article is an open-access article distributed under the terms and conditions of the Creative Commons Attribution (CC BY) license (<https://creativecommons.org/licenses/by/4.0/>), which permits unrestricted use, distribution, and reproduction in any medium, provided the original work is properly cited. The authors retain copyright of their work, and no permission is required from the authors or the publisher to reuse or distribute this article, as long as proper attribution is given to the original source.

1. Introduction

Malaria, a mosquito-borne disease, has remained a major public health scourge and development challenge. In 2020, there were 241 million malaria cases globally, 627000 of which resulted in death [1]. About 95% of these malarial deaths were in 31 countries. However, Africa has the highest malaria burden. In 2019 alone, the continent recorded 94% of the 194 million new malaria cases and 410000 deaths [2]. Malaria is one of the leading preventable causes of morbidity and mortality, but its management remains challenging due to pathogenic resistance to the currently available drugs. In addition, there are several side effects associated with the use of antimalarial drugs [3]. Thus, herbal remedies have been used in malaria prevention and treatment by indigenous communities worldwide [4, 5].

Aloe barbadensis Miller (*A. barbadensis* henceforth) is one of the 286 medicinal floras used for antimalarial therapy in rural Kenya [5-7]. In Uganda [8] and India [9], this species has also been cited for treatment of malaria. However, the antimalarial efficacy of *A. barbadensis* parts has not been exhaustively investigated [5, 9]. Aloin (Figure 1) is the phytochemical in *A. barbadensis*, which confers antimalarial activity upon it [9]. However, it is variable among species in the *Aloe* genus depending on the growing conditions of the plants [10, 11]. Recently, we reported on the intraspecific variation of the phytoconstituents, total polyphenolic content, antioxidant activity, and aloin content of *A. barbadensis* leaves across Kenya [11, 12].

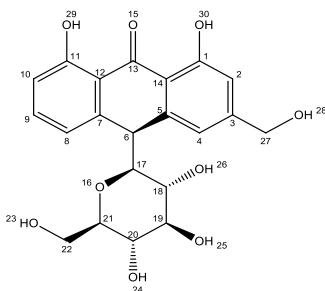


Figure 1. Chemical structure of aloin.

In continuity, the antimalarial efficacy and acute toxicity of *A. barbadensis* leaf extract, aloin (a 4-hydroxycinnamic acid-based compound), and a synthesized chitosan-Schiff base derivative of aloin isolated from this species were investigated. It was hypothesized that the derivatization of aloin using a chitosan-Schiff base derivative incorporated with 2-chloroquinoline-3-carbaldehyde could improve its stability and enhance its antimalarial effect. Chitosan is a copolymer of β -(1 \rightarrow 4)-2-acetamido-d-glucose and β -(1 \rightarrow 4)-2-amino-d-glucose obtained from deacetylated chitin found in fungal cell walls, crustacean shells, and insect exoskeletons. The amino polysaccharide (chitosan) is the second most abundant natural polymer after cellulose. It is an alkaline cationic copolymer that is biodegradable, hemostatic, mucoadhesive, and biocompatible with versatile bioactivities such as antimicrobial, antidiabetic, antiviral, anti-inflammatory, and antioxidant activities [13-15]. The chitosan-Schiff base derivative tested in the present study was obtained through superficial Schiff condensation of chitosan's amino groups with 2-chloroquinoline-3-carbaldehyde.

Quinolines, quinazolines, and their derivatives, such as 2-chloroquinoline-3-carbaldehyde proposed to be used in the present study, have distinct moieties, can be isolated from natural products, and are also available as manufactured heterocyclic compounds [14]. Drugs with quinoline skeletons (such as chloroquine, quinine, and mefloquine) are so far the best-known chemotherapeutic armory against malaria, and several derivatives of these molecules have been synthesized (through grafting, crosslinking, quaternization, and Schiff

base formation) in response to the upsurge in pathogenic resistance [15-17]. There is no report to date on the antiplasmodial activity of aloin chitosan-Schiff base scaffolds, and this study, for the first time, characterized and assessed the antimalarial efficacy and acute toxicity of a novel aloin chitosan-Schiff base scaffold.

2. Materials and Methods

2.1. Chemicals and reagents.

All the chemicals and reagents used were of analytical grade and were used without further purification. Aloin standard and 2-chloroquinoline-3-carbaldehyde were from Sigma Aldrich, Germany. The other reagents were obtained from Merck, Darmstadt, Germany. These were supplied through Centrihex Limited, Nairobi, Kenya.

2.2. Plant materials, extraction, and isolation of aloin.

Fresh *A. barbadensis* leaves were sampled in June 2021 from wild plants in Baringo County, Kenya (0°18'59.3''N 35°20'05.6''E). The extraction of phytochemicals from the latex and gels followed the protocol used by Sánchez-Machado et al. [10], with some specific modifications [11, 12]. The crude extracts thus obtained were kept at 4°C in a refrigerator until the commencement of analysis.

We attempted to isolate aloin following the precipitation method, but unexpectedly low yields were obtained. Thus, preparative thin-layer chromatography [18] was used. The exact procedures, including quantification of aloin with an authentic standard, were described in our previous study [11]. The retention factor of isolated aloin used in the synthesis (0.71) was close to that of the authentic standard (0.85). Based on high-performance liquid chromatography results, aloin from the latex had the best purity (83.79%), and it was the one used in the synthesis of the novel aloin chitosan- Schiff base scaffold.

2.3. Chemical modification of aloin.

Chitosan (0.13 g) was weighed out on a micro-analytical balance (RADWAG MYA 21.4Y.P PLUS, Rose Scientific Inc., USA). It was dissolved in a 2% acetic acid solution (20 ml) and thereafter filtered through a 0.45 µm-nylon membrane [14]. Measured 0.232 mg of 2-chloroquinoline-3-carbaldehyde was dissolved in 6 ml of ethanol. After complete dissolution, 5 ml of the dissolved 2-chloroquinoline-3-carbaldehyde was added to 10 ml of ethanol to make a volume of 15 ml. The two solutions (15 ml of chitosan and 15 ml of 2-chloroquinoline-3-carbaldehyde) were mixed and refluxed at 50°C with intermittent stirring for 6 h. The chitosan Schiff base (deep yellow gel) formed was precipitated using an excess 5% sodium hydroxide solution, filtered, and repeatedly washed with distilled water and ethanol to rid it of any 2-chloroquinoline-3-carbaldehyde that remained in solution. The resultant product was refiltered and oven-dried at 60°C.

A 0.4 mg of the synthesized yellow chitosan-Schiff base (CSB) powder was added to 0.4 mg of isolated aloin and refluxed for 3 to 6 h. Thereafter, it was concentrated by rotary evaporation and subsequently oven-dried at 35°C to obtain a yellow aloin chitosan-Schiff base derivative (ALCSB) powder.

2.4. Characterization of aloin, CSB, and ALCSB.

Prepared 10% (w/v) solutions of the isolated aloin, CSB, and ALCSB in methanol were filtered and thereafter scanned from 200 nm to 800 nm on a single beam ultraviolet-visible Beckman DU 720 UV-Vis Spectrophotometer [19]. Attenuated total reflectance Fourier-transform infrared spectroscopy (ATR-FTIR) analysis of aloin, CSB, and ALCSB was conducted using Buck Scientific 530 FTIR spectrometer (Buck Scientific Instruments LLC, Norwalk, CT, USA) at a resolution of 3 cm^{-1} from 4000 to 400 cm^{-1} . The surface morphology of aloin, CSB, and ALCSB were micrographed using an FEI Quanta 250 FEG scanning electron microscope (Thermo Fisher Scientific, Waltham, MA, USA). On the other hand, thermogravimetric analysis (TGA) and differential scanning calorimetry (DSC) analysis of aloin, CSB, and ALCSB was done using a Simultaneous Thermal Analyzer at 20 - 800°C under nitrogen at flow and heating rates of 20 mL/min and 10°C/min , respectively [20].

2.5. Assessment of antimalarial efficacy of *A. barbadensis* extract and ALCSB.

Male and female Swiss albino mice weighing 18 - 20 g were kept under a 12-hour light/dark cycle with free access to water and feeds and acclimatized for two weeks in cages. They were kept at the Animal Facility Laboratory, Mbarara University of Science and Technology, Uganda, following the Principles of Laboratory Animal Care (NIH Publication No. 85-23) [21, 22].

Plasmodium berghei NK65 (*P. berghei*) parasites were activated as per Ajayi et al. [22]. We used Peter's four-day suppressive test against chloroquine-sensitive *P. berghei* infection. Thirty-six (36) mice were randomly divided into nine groups of four each. Group I received distilled water as a negative control; groups II, III, and IV were treated with an aqueous extract; groups V, VI, and VII received ALCSB at 250 , 500 , and 1000 mg/kg/day , respectively; and groups VIII and XI (positive controls) were given chloroquine at 10 and 4 mg/kg/day , respectively. Due to low yields, aloin was excluded from testing and prioritized for stability and acute toxicity studies. Treatments were administered orally for four consecutive days, starting 3 hours post-infection. Parasitemia levels were measured on day 5 using Giemsa-stained blood smears, with percentage chemosuppression calculated from parasitized red blood cell counts in eight random fields at $\times 1000$ magnification [22].

2.6. Acute oral toxicity test.

Acute oral toxicity test followed the OECD guideline 425 [23] reported by Nureye et al. [24]. Briefly, female Swiss albino mice (fasted for 3 h and weighed) were administered increasing doses (17.5 , 55 , 175 , 550 , and 200 mg/kg bw) of the extract and ALCSB via oral gavage and further fasted for 2 h. The first mouse was observed for 30 minutes and thereafter at 4h-intervals for 1 day [24]. As neither changes in animal behavior nor mortality were recorded, four mice were administered the same dose, and they were observed for any potential toxicity signs for 14 days.

2.7. Statistical analysis.

Quantitative data from experimental replications was checked for normality using the Shapiro-Wilk test. All the data from experimental groups were included in the analysis. Data was subjected to One-Way Analysis of Variance (ANOVA) with the Tukey post hoc test (at

$P < 0.05$) to establish any significant differences among the means. The analyses and data visualizations proceeded in Origin Pro 2025a (OriginLab Corporation, Northampton, MA).

3. Results

3.1. Aloin content of *A. barbadensis* leaves.

The leaves had yields of 60.8% and 47.0% for the latex and gel, with corresponding aloin contents of 198.4 ± 2.0 mg/g and 0.36 ± 0.01 mg/g. Figure 2 shows the peaks obtained for the standard aloin (retention time = 13.589 minutes) and isolated aloin from the gel and latex extracts of *A. barbadensis* leaves (with retention times of 13.7 and 13.6 minutes, respectively).

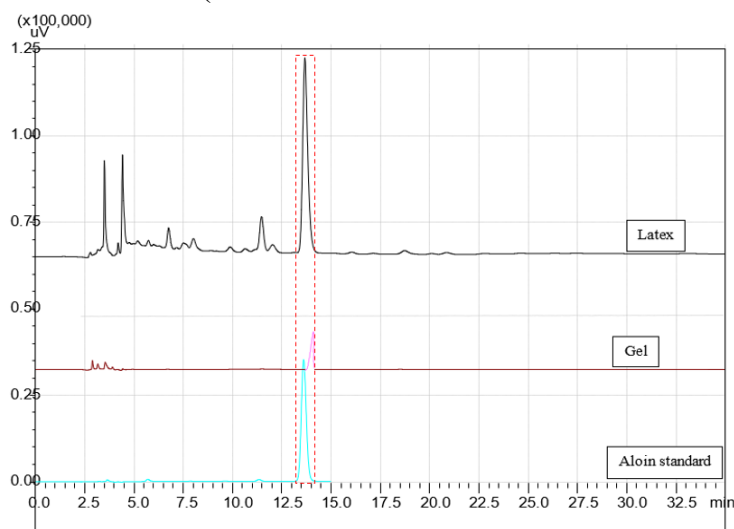


Figure 2. High-performance liquid chromatogram of aloin isolates from *A. barbadensis* leaves. Red dotted lines indicate the characteristic peaks for Aloin.

3.2. Synthesis and characterization of CSB and ALCSB.

Due to its instability, only aloin from the latex was modified using a Chitosan-Schiff base. The novel ALCSB scaffold was obtained through Schiff condensation of chitosan's amino groups and 2-chloroquinoline-3-carbaldehyde (Figure 3) [14]. One of the factors that is considered critical in syntheses involving chitosan is the degree of deacetylation, as it can directly impact the properties and applications of the chitosan derivative. For this study, some analytical techniques were used to establish whether modification of the neat chitosan to CSB and then ALCSB occurred.

The UV-Vis absorption wavelengths of aloin, CSB, and ALCSB were recorded (Figure 4). The CSB imine group showed bands with maximum absorption peaks at 285-374 nm. That of ALCSB occurred between 258 nm and 368 nm, while aloin had its absorption between 263 nm and 307 nm. Thus, saturated groups never exhibited strong absorption in the UV region. On the other hand, the FTIR spectra of CSB and ALCSB (Table 1) had similar bands but could be distinguishable by some differences in the observed intensities (for example, at 3667 cm^{-1}). Some weak bands were also present at 2936 and 2983 cm^{-1} . In ALCSB, new bands appeared between 1753 and 1765 cm^{-1} , whereas some absorption bands were also present at 1602 , 1660 , and 1590 cm^{-1} .

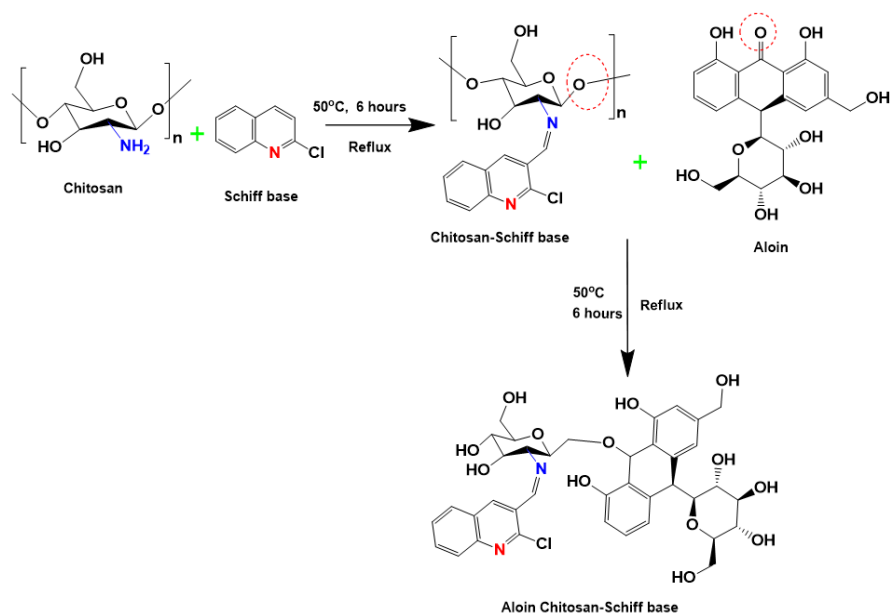


Figure 3. Proposed pathway for the synthesis of the aloin chitosan Schiff base and derivative (ALCSB), chitosan, and the Schiff base, 2-chloroquinoline-3-carbaldehyde.

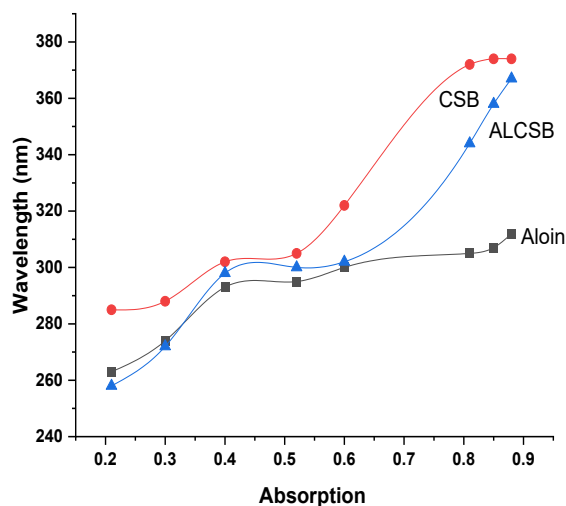


Figure 4. Maximum UV-Vis absorption wavelengths of isolated aloin, chitosan Schiff base, and alo-in-chitosan Schiff base derivative. ALCSB = aloin chitosan-Schiff base, and CSB = chitosan-Schiff base.

Table 1. ATR-FTIR functional group assignments for Aloin, CSB, and ALCSB.

Sample	Functional group and wavenumbers (cm ⁻¹)								
	O–H/N–H (Stretching)	C=N (Stretching)	C–N	C–H (Asymmetric or symmetric)	C–H (Stretching)	C=C (Aromatic)	C=O/NH (Amides)	Phenol	C–O stretch
Aloin	3622	–	–	2907	2712	1304	1661	3293	1039
Chitosan	3665	1384	2353	2964	2884	1320	1679	3593	1083
CSB	–	1393	2346	2936	2843	1347	1757	–	1115
ALCSB	3667	1405	2171	2983	2878	1660	1765	3652	1150, 1045

The UV-Vis and FTIR results pertaining to the synthesis of CSB and ALCSB were supported by scanning electron micrographs. Figures 5a and 5d show a photomicrograph of the isolated aloin from *A. barbadensis* leaf gel, which was characterized by an irregular rugged cell wall structure as compared with the fibrous and rough structure of CSB (Figures 4b and 4e) and smooth textures observed in ALCSB (Figure 5c and 5f).

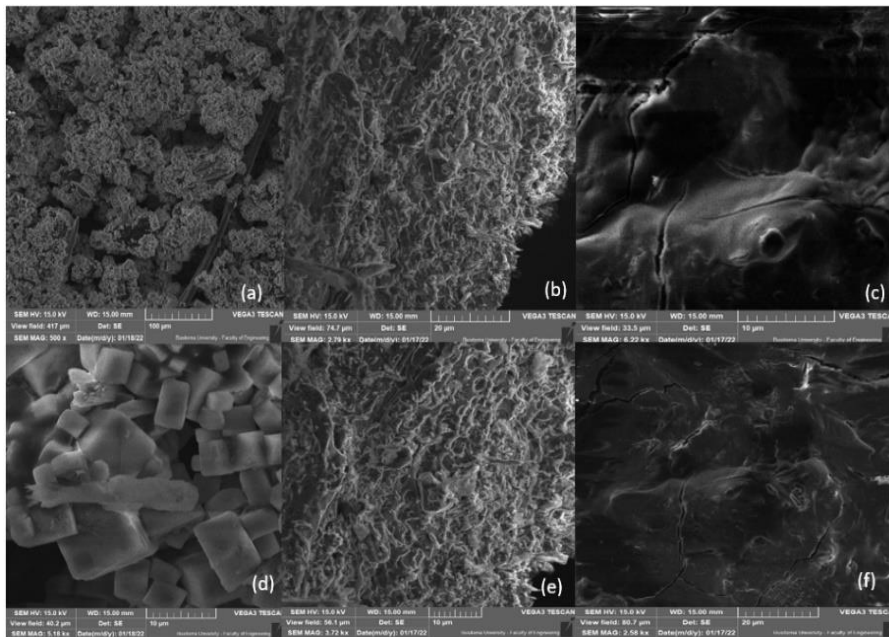


Figure 5. Scanning electron micrographs of (a) and (d) aloin; (b) and (e) chitosan Schiff base; (c) and (f) aloin-chitosan Schiff base derivative.

The thermal stability of aloin, CSB, and ALCSB expressed in terms of weight loss (Δw), and thermal degradation temperatures were further established, and the derivative thermogravimetry (DTG) curves (Figure 6) indicated that there were four different steps of mass losses.

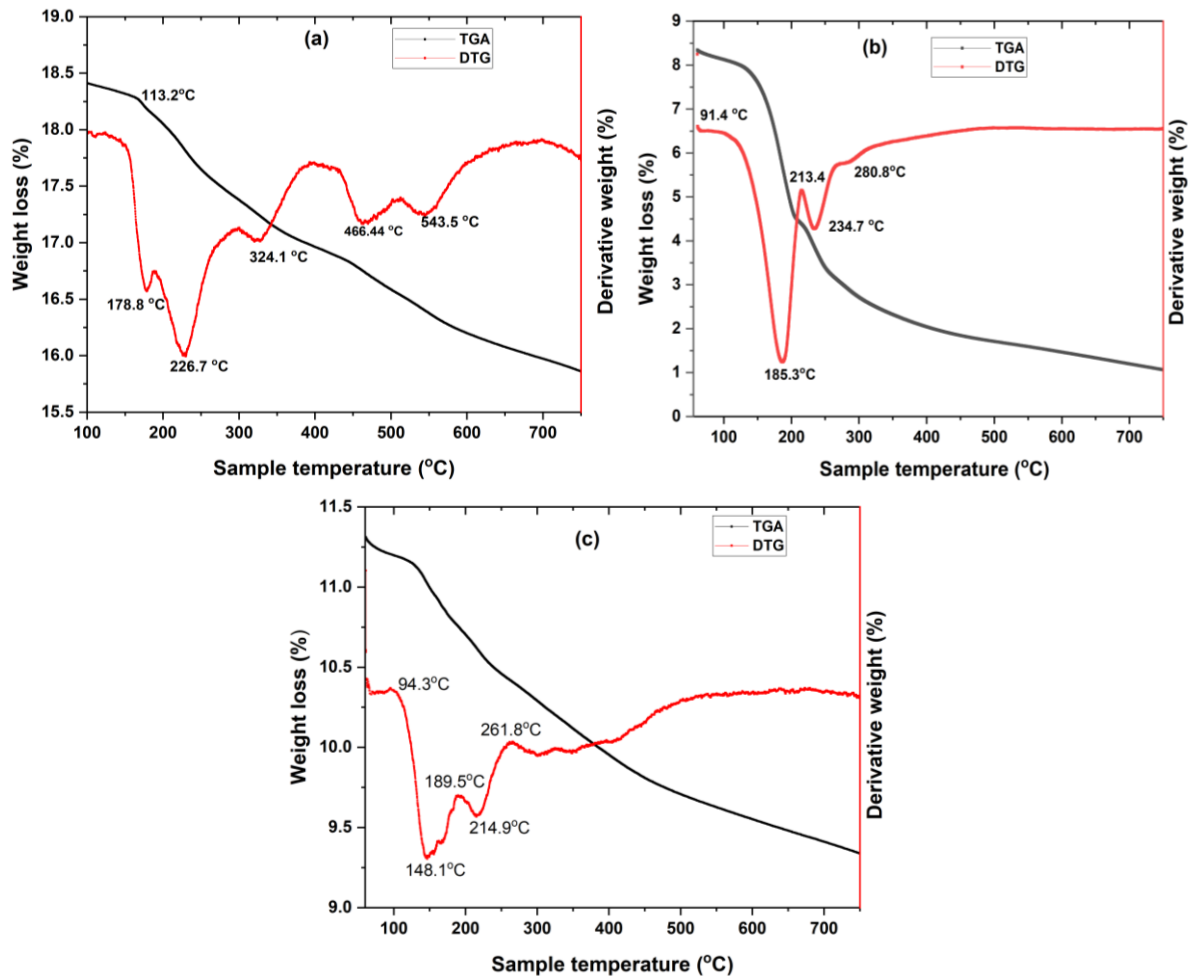


Figure 6. Thermogravimetric curves of (a) aloin; (b) chitosan-Schiff base; (c) aloin chitosan-Schiff base derivative (ALCSB).

The first step had 60.2°C and 102.4°C, 61.2°C and 148.3°C, 62.3°C and 143.6°C for aloin, CSB, and ALCSB, respectively. The second step is observed at temperatures between 173.5°C to 291.5°C, 188.6°C to 302.3°C, and 143.6°C to 214.5°C, respectively. The third step occurred at temperatures of 341.5°C to 726.4°C, 355.0°C to 751.3°C, and 347.3°C to 752.2°C, respectively.

The DTG curves agreed with the TGA curves. Aloin, CSB, and ALCSB showed four distinct transition steps of weight loss. The first weight loss occurred at 69.2°C to 129.5°C, 68.3°C to 130.5°C and 129.3°C to 147.4°C, while the second step transition was evidenced at 173.5°C, 245.5°C, 360.9°C; 174.6°C, 244.9°C and 176.4°C, 245.8°C. The third step is visible at 369.9°C, 363.2°C, and 245.8°C, 356.1°C for aloin, CSB, and ALCSB, respectively. Loss of weight during the fourth transition step occurred at 450.6°C, 547.4°C, 726.4°C; 466.3°C, 589°C and 460.4°C, and 524.7°C. Overall, the total weight losses during the transitions followed the order: aloin (20.42%) > ALCSB (19.24%) > CSB (18.96%).

3.3. *In vivo* antimalarial efficacy test results.

Aqueous extract of *A. barbadensis* leaves elicited a dose-dependent parasite reduction. On day 5 (at 250 mg/kg), there was an 8.75% parasite load reduction that differed significantly ($P < 0.05$) from the negative control group with 9.99% *P. berghei* parasitemia which further reduced to 5.70% at 1000 mg/kg (Figure 7). The extract showed better activity on day 5 with 5.95% and 4.30% parasitemia reduction at 250 mg/kg and 1000 mg/kg, respectively. There was a significant reduction of parasitemia level from that of negative control (16.89%) on day 7 post-inoculation with 8.99%, 8.53%, and 8.86% parasitemia reduction at 250 mg/kg, 500 mg/kg, and 1000 mg/kg, respectively while ALCSB showed higher parasitemia reduction of 8.87%, 5.81% and 3.99% at the same doses.

On day 5, *A. barbadensis* leaf extract showed chemosuppressive activity of 12.90 to 42.02% at 250 to 1000 mg/kg (Figure 8). However, ALCSB showed chemosuppression of 42% to 56.92% at 250 to 1000 mg/kg. There was a dose-dependent activity of ALCSB on day 7 with 79.7% activity at 1000 mg/kg in mice, although the activity significantly differed from those of the positive control group ($P < 0.01$). *A. barbadensis* leaf extract activity was 55.7% at 500 mg/kg.

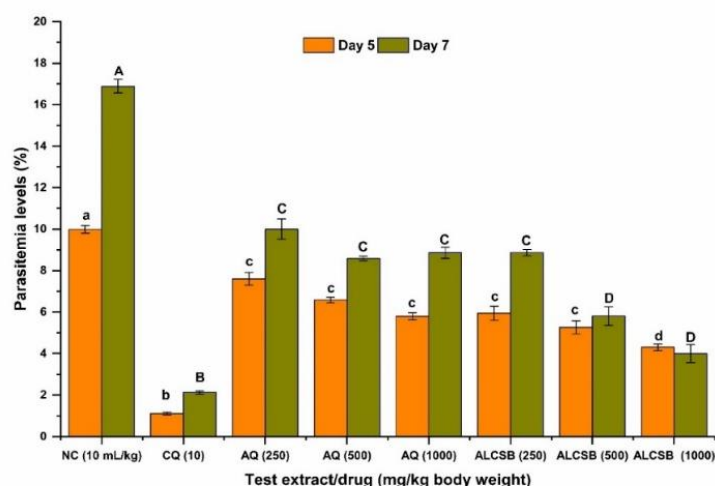


Figure 7. Parasitemia levels of *P. berghei*-infected mice dosed with *A. barbadensis* aqueous leaf extract (AQ) and ALCSB at 250 to 1000 mg/kg. NC = Negative Control, CQ = chloroquine. Bars represent standard errors of quadruplicates. Different alphabetical letters for a given day across groups indicate statistical significance at $P < 0.05$ (One-Way ANOVA).

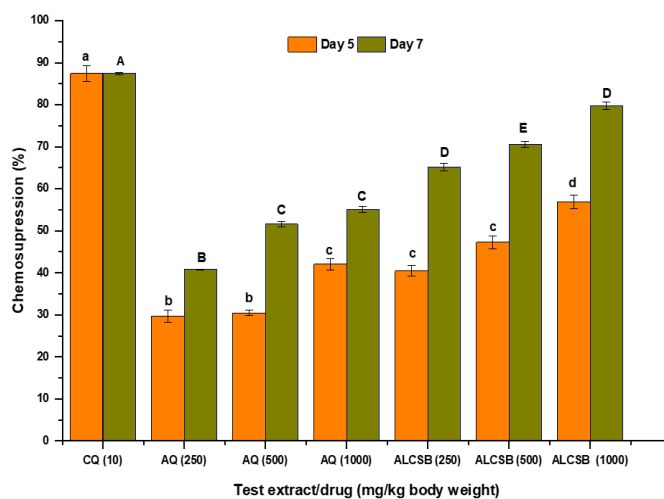


Figure 8. Chemosuppressive activities of *A. barbadensis* leaf extract (AQ) and modified aloin (ALCSB) on *P. berghei* NK65 at 250 to 1000 mg/kg. CQ = chloroquine. The extract showed no chemosuppressive activity at 250 mg/kg. Bars represent standard errors of quadruplicates. Different alphabetical letters for a given day across groups indicate statistical significance at $P < 0.01$ (One-Way ANOVA).

3.4. Acute toxicity results.

Based on the OECD guidelines, observations were a must during the first 30 minutes on the first day. They were then observed closely for the first 4 hours of each of the following days, individually in their respective cages. Signs of toxicity observed in these cases included increased motor activity, tremors, decreased motor activity, dosing, and sleeping. Both aloin and ALCSB had a median lethal dose of 1,103 mg/kg, although 11% of the mice administered with aloin at 2,000 mg/kg died within the first 6 h, indicating that it was more toxic.

4. Discussion

4.1. Characterization of aloin, CSB, and ALCSB.

The amino group of chitosan is more reactive than its hydroxyl groups. Thus, the acylation reaction proceeds preferentially on the amino group (Figure 3). In UV-Vis spectroscopy, molecules with unsaturated centers undergo $n \rightarrow \pi^*$ and $\pi \rightarrow \pi^*$ transitions; these transitions involve lesser energies and thus occur at longer wavelengths than transitions to σ^* anti-bonding orbitals spectroscopy at various concentrations, monitoring the changes in the $\pi^* - \pi^*$ and $n - \pi^*$ transitions [25]. In comparison to a previous report [18], the wavelengths (274 and 300 nm) obtained for aloin in this study (Figure 4) are close to 271 and 299 nm reported for aloin A/aloin B. This is confirmatory that the isolate was aloin.

The ATR-FTIR spectra of CSB and ALCSB illustrated typical bands for polysaccharides. For example, bands spanning from 3200 to 3400 cm^{-1} are typical of hydroxyl and amine groups [14, 26]. However, they were distinguishable by some differences in the intensity of the bands. The intensity of bands around 3667 cm^{-1} in ALCSB was assigned to OH stretching frequency. This was broad and absent in CSB [20]. The weak intensity of the band attributed to the C-H group asymmetric and asymmetric stretching bands (2936 and 2983 cm^{-1}) could also be observed in CSB and ALCSB, respectively. New bands in the region of 1757 and 1765 cm^{-1} appeared in CSB and ALCSB, corresponding to C=O stretching vibration of carbonyl products. These indicated a shift from 1661.4 and 1679.9 cm^{-1} observed in aloin and chitosan. The absorption at 1602 cm^{-1} and 1660 cm^{-1} , and 1590 cm^{-1} were assigned to C=N

vibration of imino/amide) products individually. Absorption at 1463, 1474 and 1404 cm^{-1} are due to non-symmetric and symmetric CH_2 bending, respectively. A band at 1393 cm^{-1} was attributed to ($-\text{CH}_3$) trimethyl multiplet compounds, and 1347 and 1335 cm^{-1} were assigned to C-H bend methylene compounds. Vibration bands at 1115 cm^{-1} and 1196, 1150 cm^{-1} were assigned to tertiary C-N stretch. Vibrations due to non-symmetric C–O–C stretching vibration could be observed. The strong absorption at 1045 cm^{-1} was dominated by the glycosidic linkage (C–O–C) stretching vibration contribution for ALCSB [20, 26, 27]. These fingerprint data confirmed that the synthesis of CSB and ALCSB was successful because the individual wave numbers in the initial aloin and chitosan were observed to have shifted in the synthesized compounds. For CSB, the data were in good agreement with those reported by Haj et al. [14].

For scanning electron microscopy results, the aloin surface was characterized by an irregular, rugged cell wall structure as compared with the fibrous and rough structure of CSB and smooth surfaces observed in ALCSB (Figure 5). Clearly, modification of the aloin with the CSB led to the formation of an irregular but more or less smooth morphology, which indicated the incorporation of the CSB into the aloin matrix to form the ALCSB [26, 28, 29].

The TGA and DTG curves for aloin, CSB, and ALCSB indicated that the first step of mass loss was ascribed to bound and free water [30-32]. The second step, which resulted in the maximum residual weight loss percentage, could be attributed to organic matter degradation [26, 33]. The third step occurred at temperatures of 341.5°C to 752.2°C for aloin, CSB, and ALCSB, respectively. Previous studies cited that at temperatures ranging between 290°C to 320°C, weight loss is related to the loss of major constituents with higher cross-links [32, 34]. Taken together, the order of the total weight losses during the transitions (aloin > ALCSB > CSB) suggests that ALCSB is more stable than aloin, possibly due to polymer-polymer interactions [30, 35].

4.2. Antimalarial efficacy results.

The *in vivo* antimalarial effect of the tested natural products was classified as follows: (a) at 1000 mg/kg, the antimalarial activity was considered to be moderate when the percentage growth inhibition was higher than 50%; otherwise, they were deemed inactive, (b) at 500 mg/kg, percent growth inhibition around 50% indicates moderate antimalarial activity, and (c) at 250 mg/kg, antimalarial activity was considered good if the growth inhibition was equal or greater than 50% [36].

Efficacy results for the extract in this study showed percentage inhibitions of 30.5%, 42.0%, and 40.5% for three doses (250, 500, and 1000 mg/kg, respectively) which indicated no activity because they were below 50% at day 5. On day 7, however, there were good and moderate activities (51.6%, 55%, and 65%) for 250, 500, and 100 mg/kg of the extract, respectively. ALCSB showed moderate activity at 1000 mg/kg only, while at day 7, all the doses were active, and their activity was higher than that of the extract. Considering bioactive molecules, a compound is considered an active antimalarial agent when it causes parasitemia suppression of 30% or more [37]. A previous study [9] reported half effective concentration (EC_{50} value) of 67.0 $\mu\text{g/mL}$ and 22.0 $\mu\text{g/mL}$ for antiplasmodial activity of isolated aloin and aloe-emodin from *A. barbadensis* against a chloroquine-sensitive strain of *P. falciparum* (MRC-2). In contrast with preceding reports on other *Aloe* species, an IC_{50} value of 169.76 $\mu\text{g/mL}$ for Aloin was reported against the chloroquine-sensitive 3D7 strain [38]. Recently, the leaf latex extract of *Aloe megalacantha* at 100, 200, and 400 mg/kg also had 30.3%, 43.4%, and 56.4% suppression of the parasite growth [39]. Similarly, leaf latexes of *Aloe citrina* and

Aloe pulcherrima had maximum parasite suppressions of 60.59% and 38.2% , respectively. [40, 41]. All in all, ALCSB exhibited significant antimalarial activity ($P < 0.05$), supporting that the sites that were created by the chemical modification enhanced this bioactivity.

The mechanism of action of aloin (an anthraquinone-C-glycoside) on *Plasmodium* species is not clearly understood. However, compounds with anthraquinone moiety may elicit antiplasmodial activity by inducing free radical formation in the parasite's biological systems [42] and intercalation with parasite DNA due to their cyclic planar structures [18]. Both hydroxyl (OH) and amino (NH₂) groups of chitosan are known to be the key active functional groups for its antioxidant activity and have been reported to inhibit reactive oxygen species (ROS) from donating hydrogen or lone pairs of electrons [17]. Schiff bases of heterocyclic rings with azomethine linkage, such as 2-chloroquinoline-3-carbaldehyde used in this study, are also reported to be excellent radical scavengers [43]. In addition, quinolines have a direct effect on erythrocytic schizonts (hematoschizotropic action) of *Plasmodium* species [44]. Such a combination of different possible mechanisms of action may have led to the observed enhancement in antimalarial activity. Taken together, it could be indicated that the presence of both chitosan and the Schiff base enhanced the antimalarial effect of the ALCSB.

4.3. Acute toxicity results.

In toxicity studies, none of the test mice died or showed major toxicity signs within 24 h and the next 14 days after being treated, except for those that received 2,000 mg/kg dosage. For aloin, the mice died within the first 6 h, which indicated that it was more toxic than the modified aloin, though all the two had LD₅₀ values of 1,103 mg/kg (at $P < 0.05$). Based on the OECD guideline and the analysis made, which shows that the calculated LD₅₀ of ALCSB is within the 95% confidence interval, the ALCSB is safe. Aloe Science Council standard suggests that the maximum allowable from the published literature aloin is found to be unsafe. A preceding study reported that minor signs of toxicity, such as hair erection and diarrhea, were observed in some experimental mice that received aloin isolated from *Aloe percrassa* at 2,000 mg/kg and 5,000 mg/kg [18]. Similar observations were made where no toxicity signs such as lacrimation, hair erection, and reduction in motor and feeding activities after administration of 1,500 mg/kg and 3,000 mg/kg of *Aloe debrana* leaf extract [45]. These reports support our observations in this study.

Chitosan possesses three types of reactive groups, namely, primary amine, primary, and secondary hydroxyl groups at C-2, C-3, and C-6. The primary amine at C-2 is established to be the most important group among the three reactive groups for chitosan's biological activities [14]. Chitosan has low toxicity due to its chemical and structural similarity to natural glycosaminoglycans [14]. In vivo, chitosan is readily biodegraded into harmless products (amino sugars) that can be absorbed into the body [46]. Therefore, its deacetylation and subsequent derivatization using the Schiff base and incorporation into aloin could have reduced the toxicity of aloin observed in this study.

5. Conclusions

This study synthesized an aloin-chitosan Schiff base derivative and evaluated its antimalarial efficacy and toxicity along with aloin isolated from *A. barbadensis* leaves. The derivative was successfully synthesized, as depicted by the results of UV-Vis, FTIR, scanning electron microscopy, and thermogravimetry. Chemosuppressive studies revealed that the

extract inhibited parasitemia growth, lending credence to the traditional use of *A. barbadensis* leaves for malaria treatment in Kenya. It further showed that the derivatization of aloin using a chitosan-Schiff base enhanced its antimalarial efficacy while reducing toxicity. Further studies should investigate the chemical stability of ALCSB and synthesize and test the efficacy, toxicity, and stability of other aloin-chitosan Schiff base derivatives.

Author Contributions

Conceptualization, C.K.N., V.J.K., T.O., and J.K.C.; methodology, C.K.N., V.J.K., J.O., T.O., C.O.A., and J.K.C.; software, C.K.N., and T.O.; validation, V.J.K., J.O., T.O., C.O.A., and J.K.C.; formal analysis, C.K.N.; investigation, C.K.N.; resources, C.O.A.; data curation, C.K.N., J.O., T.O., C.O.A.; writing—original draft preparation, C.K.N., and T.O.; writing—review and editing, V.J.K., J.O., C.O.A., and J.K.C.; visualization, C.K.N., and T.O.; supervision, V.J.K., J.O., and J.K.C.; funding acquisition, C.K.N., and J.K.C. All authors have read and agreed to the published version of the manuscript.

Institutional Review Board Statement

The animal study protocol was reviewed and approved by the Management Committee of the Mbarara University Animal Research Facility on 19th August 2021 (protocol code PHD/ACH/4322/20).

Informed Consent Statement

Not applicable.

Data Availability Statement

Data supporting the findings of this study are available upon reasonable request from the corresponding authors.

Funding

This research was funded by the Center of Excellence II in Phytochemicals, Textile and Renewable Energy (PTRE), Moi University (Grant No. 5798-KE).

Acknowledgments

Mbarara University of Science and Technology, Uganda, is acknowledged for the study leave and laboratory services accorded to the first author. We are grateful to Dr. Deusdedit Tusubira, the Head of Department of Mbarara University Animal Research Facility who reviewed the animal study protocol. This made the study possible despite the Ugandan government-imposed COVID-19 restrictions at the time, which allowed only a few essential organizations to remain operational.

Conflicts of Interest

The authors declare no conflict of interest.

References

1. Hollowell, T.; Sewe, M.O.; Rocklöv, J.; Obor, D.; Odhiambo, F.; Ahlm, C. Public health determinants of child malaria mortality: a surveillance study within Siaya County, Western Kenya. *Malaria J.* **2023**, *22*, 65, <https://doi.org/10.1186/s12936-023-04502-9>.
2. Tabuti, J.R.S.; Obakiro, S.B.; Nabatanzi, A.; Anywar, G.; Nambejja, C.; Mutyaba, M.R.; Omara, T.; Waako, P. Medicinal plants used for treatment of malaria by indigenous communities of Tororo District, Eastern Uganda. *Trop. Med. Health* **2023**, *51*, 34, <https://doi.org/10.1186/s41182-023-00526-8>.
3. Lai, Y.; Zhang, H.; Chen, X. Emerging trends and new developments in global research on artemisinin and its derivatives. *Heliyon* **2025**, *11*, e41086, <https://doi.org/10.1016/j.heliyon.2024.e41086>.
4. Qulsum, U.; Azad, M.T.A.; Kato, K. Efficacy of medicinal plants and their derived biomolecules against *Plasmodium falciparum*. *Parasitol. Int.* **2024**, *103*, 102946, <https://doi.org/10.1016/j.parint.2024.102946>.
5. Omara T. Antimalarial Plants Used across Kenyan Communities. *Evid Based Complement Alternat Med* **2020**, *2020*, 4538602, <https://doi.org/10.1155%2F2020%2F4538602>.
6. Nyambati, G.K.; Maranga, R.O.; Ozwara, H.; Mbugu, P.K. Use of putative antimalarial herbal medicines among communities in Trans-Mara, Kuria and Suba districts of Kenya. *SEJ Pharmacog.* **2018**, *1*, 1–14.
7. Bjorå, C.S.; Wabuyele, E.; Grace, O.M.; Nordal, I.; Newton, L.E. The uses of Kenyan aloes: an analysis of implications for names, distribution and conservation. *J. Ethnobiol. Ethnomed.* **2015**, *82*, 11, <https://doi.org/10.1186/s13002-015-0060-0>.
8. Asiimwe, S.; Namutebi, A.; Borg-Karlson, A.; Mugisha, M.; Kakudidi, E.K.; Hannington, O. Documentation and consensus of indigenous knowledge on medicinal plants used by the local communities of western Uganda. *J. Nat. Prod. Plant. Resour.* **2014**, *4*, 34–42.
9. Kumar, S.; Yadav, M.; Yadav, A.; Rohilla, P.; Yadav, J.P. Antiplasmodial potential and quantification of aloin and aloe-emodin in *Aloe vera* collected from different climatic regions of India. *BMC Compl. Alternat. Med.* **2017**, *17*, 369, <https://doi.org/10.1186/s12906-017-1883-0>.
10. Sánchez-Machado, D.I.; López-Cervantes, J.; Mariscal-Domínguez, M.F.; Cruz-Flores, P.; Campas-Baypoli, O.N.; Cantú-Soto, E.U.; Sanches-Silva, A. An HPLC procedure for the quantification of aloin in latex and gel from *Aloe barbadensis* leaves. *J. Chromatogr. Sci.* **2017**, *55*, 251–257, <https://doi.org/10.1093/chromsci/bmw179>.
11. Nakiguli, C.K.; Kosgei, V.J.; Cherutoi, J.K.; Odda, J. Quantification of aloin in *Aloe barbadensis* Miller leaf gel and latex from selected regions of Kenya. *Open Access Library J.* **2022**, *9*, e8606.
12. Nakiguli, C.K.; Kosgei, V.J.; Cherutoi, J.K.; Odda, J. Phytochemical compositions and antioxidant activity of phosphate buffered saline and aqueous extracts of *Aloe barbadensis* Miller leaf latex and gel from three counties of Kenya. *Asian J. Appl. Chem. Res.* **2022**, *11*, 17-32, <https://doi.org/10.9734/ajacr/2022/v11i130244>.
13. Richter, C.; Cord-Landwehr, S.; Singh, R.; Ryll, J.; Moerschbacher, B.M. Dissecting and optimizing bioactivities of chitosans by enzymatic modification. *Carbohydr. Polym.* **2025**, *349*, 122958, <https://doi.org/10.1016/j.carbpol.2024.122958>.
14. Haj, N.Q.; Mohammed, M.O.; Mohammad, L.E. Synthesis and Biological Evaluation of Three New Chitosan Schiff Base Derivatives. *ACS Omega.* **2020**, *5*, 13948-13954, <https://doi.org/10.1021/acsomega.0c01342>.
15. Abdel-Baky, Y.M.; Omer, A.M.; El-Fakharany, E.M.; Ammar, Y.A.; Abusaif, M.S.; Ragab, A. Developing a new multi-featured chitosan-quinoline Schiff base with potent antibacterial, antioxidant, and antidiabetic activities: design and molecular modeling simulation. *Sci. Rep.* **2023**, *13*, 22792, <https://doi.org/10.1038/s41598-023-50130-3>.
16. Touré, M.; Gassama, A.; Sambou, O.; Cavé, C.; Cojean, S. Synthesis and in vitro/in silico evaluation of the antimalarial activity of potential amino-quinoline derivatives. *Eur. J. Med. Chem. Rep.* **2025**, *13*, 100241, <https://doi.org/10.1016/j.ejmcr.2024.100241>.
17. Mostafa, M.A.; Ismail, M.M.; Morsy, J.M.; Hassanin, H.M.; Abdelrazek, M.M. Synthesis, characterization, anticancer, and antioxidant activities of chitosan Schiff bases bearing quinolinone or pyranoquinolinone and their silver nanoparticles derivatives. *Polym. Bull.* **2023**, *80*, 4035–4059, <https://doi.org/10.1007/s00289-022-04238-7>.
18. Geremedhin, G.; Bisrat, D.; Asres, K. Isolation, Characterization and in vivo Antimalarial Evaluation of Anthrones from the Leaf Latex of *Aloe percrassa* Todaro. *J. Nat. Remed.* **2014**, *14*, 119-125, <https://doi.org/10.18311/jnr/2014/72>.

19. Omara, T.; Kiprop, A.K.; Kosgei, V.J. Isolation and characterization of compounds in ethanolic extract of *Albizia coriaria* (Welw ex. Oliver) leaves: a further evidence of its ethnomedicinal diversity. *Bull. Natl. Res. Cent.* **2022**, *46*, 30, <https://doi.org/10.1186/s42269-022-00716-0>.
20. Bajer, D.; Janczak, K.; Bajer, K. Novel starch/chitosan/Aloe vera composites as promising biopackaging materials. *J. Polymers Environ.* **2020**, *28*, 1021–1039, <https://doi.org/10.1007/s10924-020-01661-7>.
21. National Research Council (US) Committee for the Update of the Guide for the Care and Use of Laboratory Animals. *Guide for the Care and Use of Laboratory Animals*, 8th Edition; The National Academies Press: Washington, D.C., **2011**.
22. Ajayi, C.O.; Elujoba, A.A.; Okella, H.; Oloro, J.; Raymond, A.; Weisheit, A.; Tolo, CU.; Ogowang, P.E. In vivo Antimalarial Activities of Five Ugandan Medicinal Plants on Plasmodium berghei in Mice. *Eur J Med Plants* **2020**, *31*, 1-13, <https://doi.org/10.9734/ejmp/2020/v31i1230300>.
23. OECD Guidelines for the Testing of Chemicals, 425: Acute Oral Toxicity—up-and-down Procedure, **2008**.
24. Nureye, D.; Sano, M.; Fekadu, M.; Duguma, T.; Tekalign, E. Antiplasmodial Activity of the Crude Extract and Solvent Fractions of Stem Barks of *Gardenia ternifolia* in Plasmodium berghei-Infected Mice. *Evid-Based Complement Altern Med.* **2021**, *2021*, 9625169, <https://doi.org/10.1155%2F2021%2F9625169>.
25. Gonciarz, A.; Pich, R.; Bogdanowicz, K.A.; Jewloszewicz, B.; Przybył, W.; Dysz, K.; Dylong, A.; Kwak, A. Kaim A, Iwan A, Rusin J, Januszko A. UV–Vis Absorption Properties of New Aromatic Imines and Their Compositions with Poly({4,8-bis[(2-Ethylhexyl)oxy]Benzo[1,2-b:4,5-b⁰]Dithiophene-2,6-diyl}{3-Fluoro-2-[(2-Ethylhexyl)Carbonyl]Thieno[3,4-b]Thiophenediyl}). *Materials* **2019**, *12*, 4191, <https://doi.org/10.3390/ma12244191>.
26. Hassan, M.A.; Omer, A.M.; Abbas, E.; Baset, W.M.A.; Tamer, T.M. Preparation, physicochemical characterization and antimicrobial activities of novel two phenolic chitosan Schiff base derivatives. *Sci. Rep.* **2018**, *8*, 11416, <https://doi.org/10.1038/s41598-018-29650-w>.
27. Tamer, T.M.; Omer, A.M.; Adel, H.M.; Hassan, M.E.; Sabet, M.M.; Eldin, M.S.M. Development of thermo-sensitive poly N-isopropyl acrylamide grafted chitosan derivatives. *J. Appl. Pharmaceut. Sci.* **2015**, *5*, 001-006, <https://dx.doi.org/10.7324/JAPS.2015.510.S1>.
28. Alesa, G.D.; Pereira Júnior, A.D.; Diniz Castro, L.; Santa Brigida, A.; Nobre Lamarão, M.L.; Ramos Barbosa, W.L.; Carréra, S.J.J.O.; Ribeiro-Costa, R.M. Polyacrylamide-Metilcellulose Hydrogels Containing Aloe barbadensis Extract as Dressing for Treatment of Chronic Cutaneous Skin Lesions. *Polymers* **2020**, *12*, 690, <https://doi.org/10.3390/polym12030690>.
29. Sali, A.; Ravi, A.P.; Shamsudeen, S.P.; Mathew, S.S.; Joseph, B.; Tharayil, A.; Vijayamma, R.; Maria, H.J.; Spatenka, P.; Kalarikkal, N.; Sabu, T. Aloe vera incorporated chitosan/nanocellulose hybrid nanocomposites as potential edible coating material under humid conditions. *J. Siberian Fed. Univ Biol.* **2021**, *14*, 475–497, <https://doi.org/10.17516/1997-1389-0366>.
30. Sánchez.; J.T.; García, A.V.; Martínez-Abad, A.; Vilaplana, F.; Jiménez, A.; Garrigós, M.C. Physicochemical and Functional Properties of Active Fish Gelatin-Based Edible Films Added with Aloe vera Gel. *Foods* **2020**, *9*, 1248, <https://doi.org/10.3390/foods9091248>.
31. Tongnuanchan, P.; Benjakul, S.; Prodpran, T. Properties and antioxidant activity of fish skin gelatin film incorporated with citrus essential oils. *Food Chem.* **2012**, *134*, 1571–1579, <https://doi.org/10.1016/j.foodchem.2012.03.094>.
32. Ali, A.M.M.; Prodpran, T.; Benjakul, S. Effect of squalene rich fraction from shark liver on mechanical, barrier and thermal properties of fish (*Probarbus jullieni*) skin gelatin film. *Food Hydrocoll.* **2019**, *96*, 123-133, <https://doi.org/10.1016/j.foodhyd.2019.05.019>.
33. Kenawy, E.R.S.; Kamoun, E.A.; Ghaly, Z.S.; Shokr, A.B.M.; El-Meligy, M.A.; Mahmoud, Y.A.G. Novel Physically Cross-Linked Curcumin-Loaded PVA/Aloe vera Hydrogel Membranes for Acceleration of Topical Wound Healing: In vitro and in vivo Experiments. *Arab. J. Sci. Eng.* **2023**, *48*, 497–514, <https://doi.org/10.1007/s13369-022-07283-6>.
34. Zhang, Y.; Simpson, B.; Dumont, M. Effect of beeswax and carnauba wax addition on properties of gelatin films: A comparative study. *Food Biosci.* **2018**, *26*, 88-95, <https://doi.org/10.1016/j.fbio.2018.09.011>.
35. Pereira, R.; Tojeira, A.; Vaz, D.C.; Mendes, A.; Bártolo, P. Preparation and characterization of films based on alginate and Aloe vera. *Int. J. Polymer Anal. Charact.* **2011**, *16*, 449–464, <https://doi.org/10.1080/1023666X.2011.599923>.
36. Muñoz, V.; Sauvain, M.; Bourdy, G.; Arrázola, S.; Callapa, J.; Ruiz, G.; Choque, J.; Deharo, E. A search for natural bioactive compounds in Bolivia through a multidisciplinary approach. Part III. Evaluation Of the

- antimalarial activity of plants used by Alteños Indians. *J. Ethnopharmacol.* **2000**, *71*, 123-31, [https://doi.org/10.1016/s0378-8741\(99\)00191-9](https://doi.org/10.1016/s0378-8741(99)00191-9).
37. Krettli, A.U.; Adebayo, J.O.; Krettli, L.G. Testing of natural products and synthetic molecules aiming at new antimalarials. *Curr. Drug Targets* **2009**, *10*, 261-70, <https://doi.org/10.2174/138945009787581203>.
 38. Van Zyl, R.; Viljoen, A. In vitro activity of Aloe extracts against *Plasmodium falciparum*. *South Afr. J. Bot.* **2002**, *68*, 106–10, [https://doi.org/10.1016/S0254-6299\(15\)30451-8](https://doi.org/10.1016/S0254-6299(15)30451-8).
 39. Hintsä, G.; Sibhat, G.G.; Karim, A. Evaluation of Antimalarial Activity of the Leaf Latex and TLC Isolates from *Aloe megalacantha* Baker in *Plasmodium berghei* Infected Mice. *Evid-based Complement. Altern. Med.* **2019**, *2019*, 6459498, <https://doi.org/10.1155/2019/6459498>.
 40. Girma, B.; Bisrat, D.; Asres, K. Antimalarial evaluation of the leaf latex of *Aloe citrina* and its major constituent. *Anc. Sci. Life.* **2015**, *34*, 142-146, <https://doi.org/10.4103/0257-7941.157158>.
 41. Tekka, T.; Bisrat, D.; Yeshak, M.Y.; Asres, K. Antimalarial Activity of the Chemical Constituents of the Leaf Latex of *Aloe pulcherrima* Gilbert and Sebsebe. *Molecules* **2016**, *21*, 1415, <https://doi.org/10.3390/molecules21111415>.
 42. Osman, C.P.; Ismail, N.H. Antiplasmodial anthraquinones from medicinal plants: The chemistry and possible mode of actions. *Natural Product Communications* **2018**, *13*, 1934578X1801301207, <https://doi.org/10.1177/1934578X1801301207>.
 43. Sullivan, D.J. *Plasmodium* drug targets outside the genetic control of the parasite. *Curr. Pharm. Design* **2013**, *19*, 282–289, <http://dx.doi.org/10.2174/1381612811306020282>.
 44. Deressa, T.; Mekonnen, Y.; Animut, A. In vivo anti-malarial activities of *Clerodendrum myricoides*, *Dodonea angustifolia* and *Aloe debrana* against *Plasmodium berghei*. *Ethiopian J. Health Dev.* **2010**, *24*, 25-28, <https://doi.org/10.4314/ejhd.v24i1.62941>.
 45. Kumar, M.; Padmini, T.; Ponnuvel, K. Synthesis, characterization, and antioxidant activities of Schiff bases are of cholesterol. *J. Saudi Chem. Soc.* **2017**, *21*, S322–S328, <https://doi.org/10.1016/j.jscs.2014.03.006>.
 46. Sonia, T.A.; Sharma, C.P. Chitosan and Its Derivatives for Drug Delivery Perspective. In *Chitosan for Biomaterials I*, Jayakumar, R., Prabakaran, M., Muzzarelli, R.A.A., Eds.; Springer Berlin Heidelberg: Berlin, Heidelberg, **2011**; Volume 243, pp. 23-53, https://doi.org/10.1007/12_2011_117.

Publisher's Note & Disclaimer

The statements, opinions, and data presented in this publication are solely those of the individual author(s) and contributor(s) and do not necessarily reflect the views of the publisher and/or the editor(s). The publisher and/or the editor(s) disclaim any responsibility for the accuracy, completeness, or reliability of the content. Neither the publisher nor the editor(s) assume any legal liability for any errors, omissions, or consequences arising from the use of the information presented in this publication. Furthermore, the publisher and/or the editor(s) disclaim any liability for any injury, damage, or loss to persons or property that may result from the use of any ideas, methods, instructions, or products mentioned in the content. Readers are encouraged to independently verify any information before relying on it, and the publisher assumes no responsibility for any consequences arising from the use of materials contained in this publication.